

Quantum simulations of the Abelian Higgs model

Alexei Bazavov¹ and Yannick Meurice²

¹ Michigan State University

² University of Iowa

arXiv:1803.11166

Work done with Shan-Wen Tsai (UCR), Judah Unmuth-Yockey (U. Iowa/Syracuse), and Jin Zhang (UCR)

ANL, 3/29/18

- Motivations from the lattice gauge theory point of view
- The Abelian Higgs model on a 1+1 lattice (PRD 92, 076003)
- The Hamiltonian
- Data collapse for Polyakov's loop (arXiv:1803.11166)
- Ladders of Rydberg atoms
- A proof of principle: data collapse for the quantum Ising model
- Conclusions

Motivations for quantum simulations in lattice gauge theory and high energy physics

- Lattice QCD has been very successful at establishing that QCD is the theory of strong interactions, however some aspects remain inaccessible to classical computing.
- **Finite density calculations**: sign problem (MC calculations with complex actions are only possible if the complex part is small enough to be handled with reweighing). Relevant for heavy ion collisions.
- **Real time evolution**: requires detailed information about the Hamiltonian and the states which is usually not available from conventional MC simulations at Euclidean time. Collider jet physics from first principles?
- Quantum simulations with optical lattices were successful in Condensed Matter (Bose-Hubbard), but **so far no actual implementations for lattice gauge theory**

The Abelian Higgs model on a 1+1 space-time lattice

a.k.a. lattice **scalar electrodynamics**. Field content:

- **Complex (charged) scalar field** $\phi_x = |\phi_x|e^{i\theta_x}$ on space-time sites x
- **Abelian gauge fields** $U_{x,\mu} = \exp iA_\mu(x)$ on the links from x to $x + \hat{\mu}$
- $F_{\mu\nu}F^{\mu\nu}$ appears in products of U 's around a **plaquette** in the $\mu\nu$ plane: $U_{x,\mu\nu} = e^{i(A_\mu(x)+A_\nu(x+\hat{\mu})-A_\mu(x+\hat{\nu})-A_\nu(x))}$
- $\beta_{pl.} = 1/g^2$, g is the **gauge coupling** and κ is the **hopping** coefficient

$$\begin{aligned} S = & -\beta_{pl.} \sum_x \sum_{\nu < \mu} \text{ReTr} [U_{x,\mu\nu}] + \lambda \sum_x \left(\phi_x^\dagger \phi_x - 1 \right)^2 + \sum_x \phi_x^\dagger \phi_x \\ & - \kappa \sum_x \sum_{\nu=1}^d \left[e^{\mu_{ch.} \delta(\nu,t)} \phi_x^\dagger U_{x,\nu} \phi_{x+\hat{\nu}} + e^{-\mu_{ch.} \delta(\nu,t)} \phi_{x+\hat{\nu}}^\dagger U_{x,\nu}^\dagger \phi_x \right]. \end{aligned}$$

$$Z = \int D\phi^\dagger D\phi D U e^{-S}$$

Unlike other approaches (Reznik, Zohar, Cirac, Lewenstein, Kuno,...) we will not try to implement the gauge field on the optical lattice.



The large λ limit (finite λ will not be considered here)

- $\lambda \rightarrow \infty$, $|\phi_x|$ is frozen to 1, or in other words, the Brout-Englert-Higgs mode becomes infinitely massive.
- We are then left with **compact variables** of integration in the original formulation (θ_x and $A_{x,\hat{\nu}}$) and the **discrete** Fourier expansions $\exp[2\kappa_{\hat{\nu}} \cos(\theta_{x+\hat{\nu}} - \theta_x + A_{x,\hat{\nu}})] = \sum_{n=-\infty}^{\infty} I_n(2\kappa_{\hat{\nu}}) \exp(in(\theta_{x+\hat{\nu}} - \theta_x + A_{x,\hat{\nu}}))$
- This leads to **expressions of the partition function in terms of discrete sums. This is important for quantum computing.**
- When $g = 0$ we recover the $O(2)$ model (KT transition)

We use the following definitions:

$$t_n(z) \equiv I_n(z)/I_0(z)$$

For z non zero and finite, we have $1 > t_0(z) > t_1(z) > t_2(z) > \dots > 0$

In addition for sufficiently large z ,

$t_n(z) \simeq 1 - n^2/(2z)$ will be used to take the time continuum limit



Tensor Renormalization Group formulation

As in PRD.88.056005 and PRD.92.076003, we attach a $B^{(\square)}$ tensor to every plaquette

$$B_{m_1 m_2 m_3 m_4}^{(\square)} = \begin{cases} t_{m_{\square}}(\beta_{pl}), & \text{if } m_1 = m_2 = m_3 = m_4 = m_{\square} \\ 0, & \text{otherwise.} \end{cases}$$

a $A^{(s)}$ tensor to the horizontal links

$$A_{m_{up} m_{down}}^{(s)} = t_{|m_{down} - m_{up}|}(2\kappa_s),$$

and a $A^{(\tau)}$ tensor to the vertical links

$$A_{m_{left} m_{right}}^{(\tau)} = t_{|m_{left} - m_{right}|}(2\kappa_{\tau}) e^{\mu}.$$

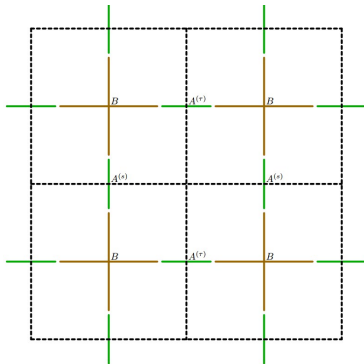
The quantum numbers on the links are completely determined by the quantum numbers on the plaquettes



$$Z = \text{Tr}[\prod T]$$

$$Z = \propto \text{Tr} \left[\prod_{h,v,\square} A_{m_{up}m_{down}}^{(s)} A_{m_{right}m_{left}}^{(\tau)} B_{m_1m_2m_3m_4}^{(\square)} \right] .$$

The traces are performed by contracting the indices as shown



The Hamiltonian (time continuum limit)

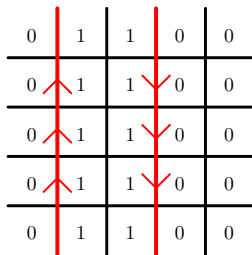
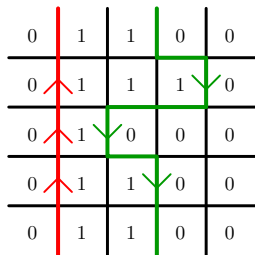
- For $1 \ll \beta_{pl} \ll \kappa_\tau$, we obtain the time continuum limit.
- For practical implementation, we need a truncation of the plaquette quantum number ("finite spin")
- We use the notation $\bar{L}_{(i)}^x$ to denote a matrix with equal matrix elements on the first off-diagonal (like the first generator of the rotation algebra in the spin-1 representation)
- Parameters: $\tilde{Y} \equiv (\beta_{pl}/(2\kappa_\tau))\tilde{U}_g$ and $\tilde{X} \equiv (\beta_{pl}\kappa_s\sqrt{2})\tilde{U}_g$ which are the (small) energy scales.
- The final form of the Hamiltonian \bar{H} is

$$\bar{H} = \frac{\tilde{U}_g}{2} \sum_i \left(\bar{L}_{(i)}^z \right)^2 + \frac{\tilde{Y}}{2} \sum_i \left(\bar{L}_{(i)}^z - \bar{L}_{(i+1)}^z \right)^2 - \tilde{X} \sum_i \bar{L}_{(i)}^x .$$

Polyakov loop: definition

Polyakov loop, a Wilson line wrapping around the Euclidean time direction: $\langle P_i \rangle = \langle \prod_j U_{(i,j),\tau} \rangle = \exp(-F(\text{single charge})/kT)$; the order parameter for deconfinement.

With periodic boundary condition, the insertion of the Polyakov loop (red) forces the presence of a scalar current (green) in the opposite direction (left) or another Polyakov loop (right).



In the Hamiltonian formulation, we add $-\frac{\tilde{\gamma}}{2}(2(\bar{L}_{i^*}^Z - \bar{L}_{(i^*+1)}^Z) - 1)$ to H .

Expectations

- $|\langle P \rangle| \propto e^{-N_\tau \Delta E}$, with ΔE the gap between the neutral and charge 1 ground states.
- For κ (or \tilde{X}) large enough and $g^2 N_s$ small enough:

$$\Delta E \simeq a/N_s + bg^2 N_s$$

(KT phase when $g = 0$ and a linear gauge potential)

- $\Delta E N_s = f(g^2 N_s^2)$ (data collapse related to KT)? This would be great because it works for small volumes
- For larger $g^2 N_s^2$, $f(g^2 N_s^2) \sim \sqrt{g^2 N_s^2}$, so ΔE stabilizes at large N_s at some value proportional to g (for fixed g).
- The Polyakov loop can be replaced by 1-0 boundary conditions (to create a charge 1 state).

Polyakov loop collapse (Judah Unmuth-Yockey)

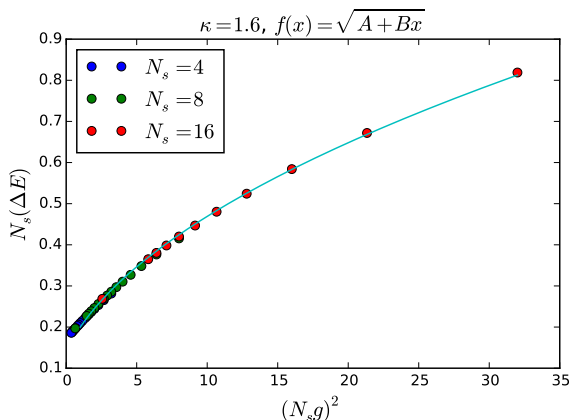


Figure: A fit to the universal curve of the form $\sqrt{A + Bx}$. In this calculation, space and Euclidean time are treated isotropically.

Polyakov loop collapse (Jin Zhang)

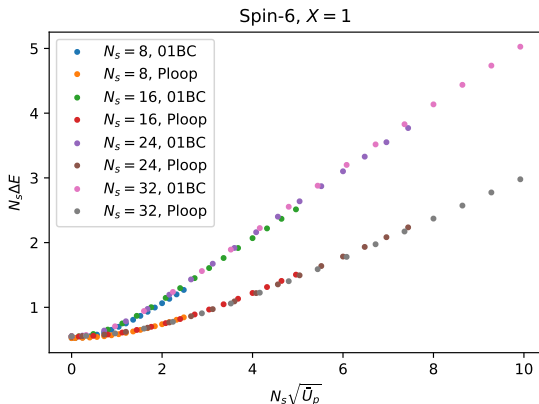


Figure: Same data collapse with the Hamiltonian formulation: we add $-\frac{\tilde{Y}}{2}(2(\bar{L}_{i^*}^z - \bar{L}_{(i^*+1)}^z) - 1)$ to H (lower set), or with 0-1 boundary conditions (upper set).

Universal functions I: the Polyakov loop

Today's posting: arXiv:1803.11166

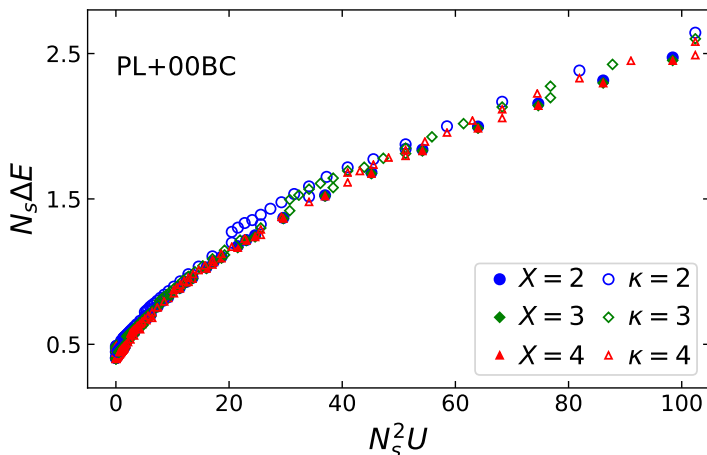


Figure: Data collapse of $N_s \Delta E$ defined from the insertion of the Polyakov loop, as a function of $N_s^2 U$, or $(N_s g)^2$ (collapse of 24 datasets).

Universal functions II: Background field (1803.11166)

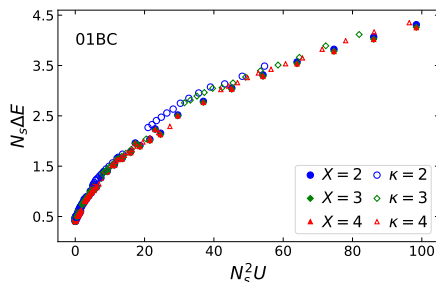


Figure: The data collapse of $N_s \Delta E$ as a function of $N_s^2 U$, or $(N_s g)^2$, for three different values of X , or κ , in both the isotropic coupling, and continuous time limits. Four different system sizes were used: $N_s = 4, 8, 16$, and 32 . The solid markers are data obtained from DMRG calculations done in the Hamiltonian limit, while empty markers are data taken from HOTRG calculations done in the Lagrangian limit. ΔE is the difference in the ground state energies between a system with zero and one on the boundaries, and a system with open boundary conditions (zeros on the boundaries). The isotropic data has been rescaled by 2κ on both axes.

Collapse breaking: small N_s , large g_{gauge} (P. loop)

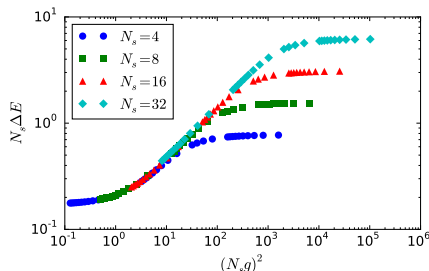


Figure: A plot showing the data collapse across different N_s for sufficiently small g , and collapse breaking across different N_s at large g in the case of isotropic coupling. Here $\kappa = 1.6$, and $D_{\text{bond}} = 41$ was used in the HOTRG calculations.

Collapse breaking: small N_s , large g_{gauge} (E field)

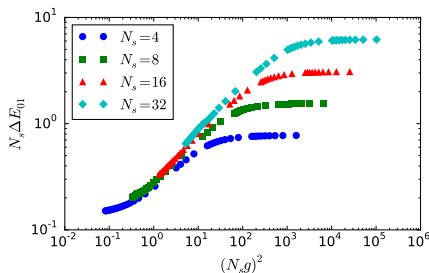


Figure: The energy gap between the 01-boundary condition partition function and the 00-boundary condition (typical open boundary condition) partition function in the case of isotropic coupling. This is for $\kappa = 1.6$ and $D_{\text{bond}} = 41$ for the HOTRG truncation. Similar to the Polyakov loop gap, for sufficiently small g we see data collapse, and for g large enough we see the collapse breakdown.

Optical lattice implementation with a ladder

$$\bar{H} = \frac{\tilde{U}_g}{2} \sum_i \left(\bar{L}_{(i)}^z \right)^2 + \frac{\tilde{Y}}{2} \sum_i \left(\bar{L}_{(i)}^z - \bar{L}_{(i+1)}^z \right)^2 - \tilde{X} \sum_i \bar{L}_{(i)}^x$$

5 states ladder with 9 rungs

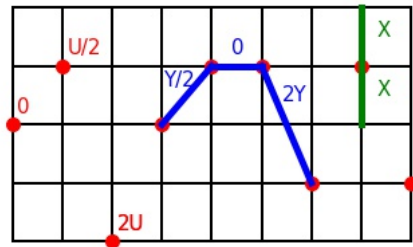
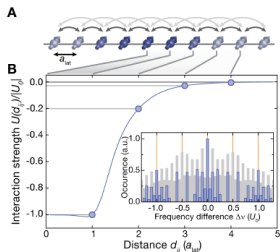


Figure: Ladder with one atom per rung: tunneling along the vertical direction, no tunneling in the horizontal direction but short range attractive interactions. A parabolic potential is applied in the spin (vertical) direction.

Recent experimental progress



High-resolution detection

Quantum gas microscopes enable the high-resolution fluorescence detection of atoms in single sites of a two-dimensional layer of optical lattices. The lattice spacing is small (typically $0.5\ \mu\text{m}$), such that the atoms can move through the lattice by tunneling with amplitude t . Additionally, they interact with each other with strength U when multiple atoms meet at the same lattice site. Quantum gas microscopy can provide access to single snapshots of the locally resolved atomic density in strongly correlated many-body systems.

A typical fluorescence image is shown at the lower left, where the fluorescence strength is encoded in the color scale from black over red to yellow. Thanks to the underlying lattice (white dots), the single site occupation can be faithfully reconstructed even in dense areas, whereas sparse individual atoms are directly visible.

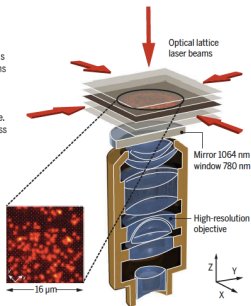


Fig. 1 Quantum gas microscopes. [Adapted from (20)]

Tunable nearest neighbor interactions, Johannes Zeiher et al. arxiv 1705.08372

Quantum gas microscopes, Gross and Bloch, Science 357, 995-1001 (2017)

A first quantum calculator for the abelian Higgs model?

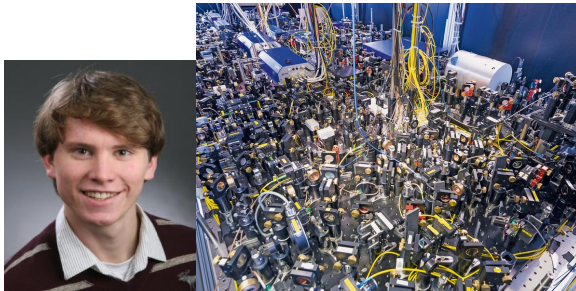


Figure: Left: Johannes Zeiher, a recent graduate from Immanuel Bloch's group can design ladder shaped optical lattices with nearest neighbor interactions. Right: an optical lattice experiment of Bloch's group.

The quantum Ising model

In the case of 2 long sides (spin 1/2), we recover the quantum Ising model:

$$\hat{H} = -\lambda \sum_i \hat{\sigma}_i^z \hat{\sigma}_{i+1}^z - \sum_i \hat{\sigma}_i^x - h \sum_i \hat{\sigma}_i^z$$

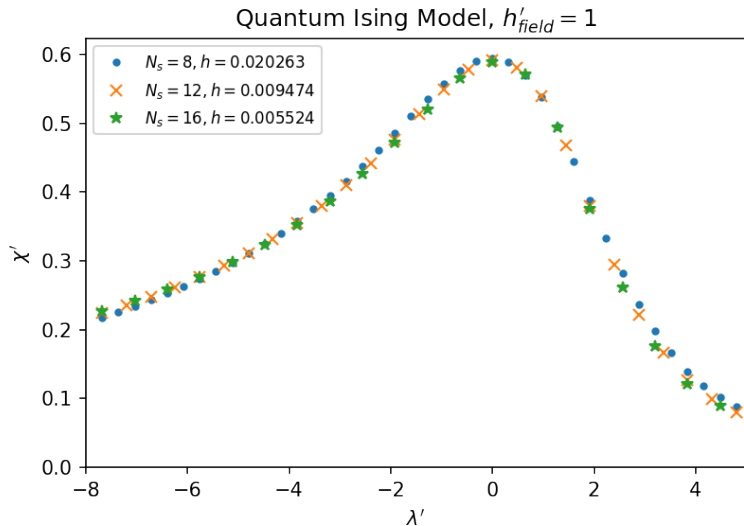
where all the energies are expressed in units of the transverse magnetic field (the coefficient in front of $-\sum_i \hat{\sigma}_i^x$). In the ladder realization, this is proportional to the inverse tunneling time along the rungs. The zero temperature magnetic susceptibility is

$$\chi^{quant.} = \frac{1}{L} \sum_{\langle i,j \rangle} \langle (\sigma_i - \langle \sigma_i \rangle) (\sigma_j - \langle \sigma_j \rangle) \rangle \propto \xi^{1-\eta} \propto |\lambda - 1|^{-\nu(1-\eta)}$$

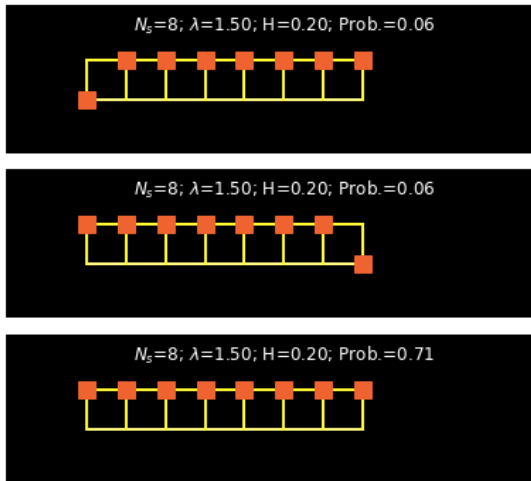
where $\langle \dots \rangle$ are short notations for $\langle \Omega | \dots | \Omega \rangle$ with $|\Omega\rangle$ the lowest energy state of \hat{H} . Recent calculations by Jin Zhang show a nice data collapse.

Data collapse for the quantum magnetic susceptibility:

$$\chi^{quant.'} = \chi^{quant.} L^{-(1-\eta)}, \lambda' = L^{1/\nu}(\lambda - 1), h' = hL^{15/8}$$



Looking at the vacuum wavefunction: σ^z meas. Could we replace the rungs by q-bits?



Conclusions

- We have proposed a **gauge-invariant** approach for the quantum simulation of the abelian Higgs model.
- The tensor renormalization group approach provides a discrete formulation in the limit $\lambda \rightarrow \infty$ (suitable for quantum computing)
- Calculations of the **Polyakov loop** at finite N_x and small gauge coupling show a universal behavior (collapse related to the KT transition of the limiting $O(2)$ model).
- A ladder of cold atoms with N_s rungs, one atom per rung, and $2s + 1$ long sides seems to be the most promising realization
- Spin truncations can affect the collapse (not discussed here)
- Proof of principle: data collapse for the quantum Ising model.
- D-wave machine realization?
- Thanks for listening!

Acknowledgements:

This research was supported in part by the Dept. of Energy under Award Numbers DOE grants DE-SC0010114, DE-SC0010113, and DE-SC0013496 and the NSF under grant DMR-1411345.